Pilot-Scale Experimental Study on the CO2 Capture Process with Existing of SO2: Degradation, Reaction Rate, and Mass Transfer

ARTICLE *in* ENERGY & FUELS · NOVEMBER 2011

Impact Factor: 2.79 · DOI: 10.1021/ef2010496

energy&fuels

ARTICLE

pubs.acs.org/EF

Pilot-Scale Experimental Study on the CO_2 Capture Process with Existing of SO_2: Degradation, Reaction Rate, and Mass Transfer

Jubao Gao, Shujuan Wang,* Bo Zhao, Guojie Qi, and Changhe Chen

Key Laboratory for Thermal Science and Power Engineering of Ministry of Education Department of Thermal Engineering, Tsinghua University, Beijing 100084, China

ABSTRACT: A lab amine-based chemical absorption pilot plant for CO_2 capture from coal-fired power plants was built. The character of CO_2 capture of the new blended amine absorbent was studied in the pilot plant, under the condition of prolonged operation. Three campaigns were conducted. One campaign was the baseline experiment to evaluate the cyclic absorption and desorption character of the absorbent during 500 h with 12 vol % CO_2 and 18 vol % O_2. Other two campaigns were performed to evaluate the influence of SO_2 on the absorption character of the absorbent, with 214 and 317 ppm SO_2, respectively. The CO_2 reaction rate and mass transfer behavior were analyzed for the three campaigns. The results show that the CO_2 removal efficiency is in inverse proportion to reaction time, and the results of amine degradation and heat stable salts formation are in accordance with it. The SO_2 removal efficiency is almost 100%. After the addition of SO_2 to the simulated flue gas, there is more serious amine degradation and more heat stable salts formation. Four kinds of organic acid salts, such as formate, acetate, oxalate, and glycolate, were detected with and without SO_2. The analysis on mass transfer and CO_2 reaction rate indicates that the free amine concentration reduction is the main reason for the CO_2 removal efficiency decreases. The combination of SO_2 with amine results in the decrease in free amines.

1. INTRODUCTION

It is well recognized that greenhouse gases, such as CO_2, CH_4, N_2O, HFCS, PFCS, and SF_6, contribute to global warming and climate change. Among these greenhouse gases, anthropogenic carbon dioxide from fossil fuel is the most important one because of its long life and large amount.[1] Power plants, cement plants, steel plants, and refinery plants are all concentrated sources of carbon dioxide. The emission of CO_2 from fossil fuel-fired power plants accounts for above 30% of the total. Thus, the CO_2 capture from fossil fuel-fired power plants is of wide concern. Many technologies may be used to separate CO_2 from flue gas, such as amine scrubbing, carbonation−calcination recycle technology (CCR), O_2/CO_2 recycle combustion technology, and chemical-looping combustion technology (CLC).[2−6] The amine-based technology is the only commercially available one.

In effect, amine-based scrubbing technology has been used to separate carbon dioxide from natural gas in the chemical industry for several decades. Although many problems, such as high energy consumption and corrosion, occur with amine scrubbing of flue gas from fossil fuel-fired power plants, amine-based scrubbing technology is still as timely solution for postcombustion CO_2 capture, compared other advanced technologies.[7]The flue gas from coal-fired power plants, however, with characteristics of large flow rate, high temperature, low CO_2 partial pressure, and containing SO_2, NO_x, and fly ash, is quite different from that from natural gas. Therefore, the technology must be further studied according to the conditions of coal-fired power plants.

The most widely used amines for CO_2 capture include monoethanolamine (MEA), diethanolamine (DEA), and methyldiethanolamine (MDEA). MEA was widely used to absorb CO_2 for its fast reaction rate. The disadvantages of using MEA are its high energy requirement and corrosion, and the chemical stability of the solvent is very important to maintain a small energy requirement.[8] Hence, many new single and blended amines were studied as replaceable absorbents.[9] As to the amine chemical stability, Uyanga and Idem studied the SO_2 induced degradation of aqueous MEA using a semibatch reactor.[10] Degradation pathways for MEA were studied by Strazisar and Anderson, using degraded MEA samples from a chemicals facility.[11]

Although there is substantial information on new amines and their chemical stability, the information on the effects of SO_2 on the CO_2 capture processes and its kinetic performance are scant. A novel solvent specified by Toshiba was used to capture CO_2 in the pilot plant. The SO_2 was added to evaluate its effect on the CO_2 capture processes. The reaction rate and mass transfer were also analyzed for three campaigns in this work.

2. EXPERIMENTAL SECTION

2.1. Materials. N_2, O_2, CO_2, and SO_2 with more than 99.9% concentration were used to simulate coal-fired flue gas. The chemical reagents are industry grade, with concentrations of more than 98%. The blended amine solvent specified by Toshiba was used in this research work. It contains a tertiary amine and additives to promote the amine.

2.2. Analysis Methods. The CO_2 concentrations at the absorber inlet and outlet were recorded by an IR CO_2 analyzer (China Huayun Company) and range from 0 to 20% and 0 to 5%, respectively. The SO_2 flow rate was controlled by a mass flow controller and was continuously added to the whole system. A SO_2 IR analyzer (Thermo Company) was used to analyze the SO_2 concentration. Meanwhile, the O_2 concentration was detected by a paramagnetic oxygen-meter. Dionex ICS-1000

Received: August 8, 2011
Revised: October 17, 2011
Published: October 18, 2011

and DX120 ion chromatographic instruments were used to analyze the anions and cations, respectively. The CO_2 loading was determined by a total organic carbon analyzer (TOC-5000, Shimadzu). The solution viscosity was measured by a viscometer (SV-10, AND).

2.3. Pilot-Scale Plant. Figure 1 shows the scheme of the small loop pilot plant for CO_2 absorption and desorption using an aqueous blended amine solvent built in Tsinghua University, which is same as a conventional amine-based CO_2 recovery plant except for recycled flue gas. No fresh solvent and water was added into the system during the campaign; therefore, this design can keep water balance. The absorber and the stripper, with an internal diameter of 0.207 m, were filled with 700Y gauze-structured, 3-m height stainless steel packing. The major equipment and pipeline are made of 316 L stainless steel. The heat input to the stripper is supplied by electrical heater with the power of 60 kW. Liquid samples for composition testing were collected per 100 h during the operation. The plant can be operated continuously, and all the testing data can be recorded automatically.

2.4. Operating Conditions. Three campaigns have been conducted in this pilot plant. Some important parameters are shown in Table 1. The flue gas of campaign 1 contains about 12 vol % CO_2 and 18 vol % O_2. The experimental conditions of the campaign 2 and campaign 3 were identical to those of campaign 1, excluding adding SO_2 with concentrations of 214 and 317 ppm, respectively. The average flue gas flow rate of the three campaigns was about 86 N m^3/h, and the average liquid solvent flow rate was around 0.6 m^3/h. The average temperatures at the bottom of the absorber and the stripper were 46 and 116 °C, respectively. The continuous operating time was around 500 h for campaign 1, 430 h for campaign 2, and 345 h for campaign 3. If the CO_2 removal efficiency was less than 60% or the CO_2 concentration out of the absorber reached 5%, which is the maximum value of analyzer, the campaign was stopped. Hence, the operating time of the last two campaigns was short.

3. RESULTS AND DISCUSSION

3.1. CO_2 and SO_2 Removal Efficiency. The removal efficiency was calculated from the difference between the amounts of CO_2 entering and leaving the absorption column, which can be expressed by the following equation:[12]

$$\eta_{CO_2} = \frac{C_{in} - C_{out}}{C_{in}(1 - C_{out})} \quad (1)$$

where C_{in} and C_{out} denote volume fractions of gas CO_2 entering and leaving the absorber, respectively.

According to Figure 2, the CO_2 removal efficiency decreases gradually as circulating time increases. The increase in the SO_2 concentration obviously has an impact on the CO_2 removal efficiency. Logically, CO_2 is absorbed by the amine solution following two steps, diffusion from gas bulk to liquid bulk and chemical reaction at the gas−liquid interface or in the liquid bulk. The overall CO_2 reaction rate can be expressed as[13,14]

$$r_{ov} = k_{am}[AM][CO_2] + k_{OH^-}[OH^-][CO_2] \quad (2)$$

Therefore, the amine concentration has an important effect on the overall CO_2 reaction rate and then on the CO_2 removal efficiency.

SO_2 was continuously fed into the bottom of the absorber during the last two campaigns. The SO_2 concentration out of the absorber was recorded per 12 h, and the inlet SO_2 concentration was controlled precisely by a mass flow controller. The SO_2 concentration at the inlet and outlet of the absorber is shown in Figure 3. Comparing campaign 3 and campaign 2, the outlet SO_2 concentration was dramatically increased with the increasing SO_2 concentration. The maximum value of which, however, was still very small compared with the inlet SO_2 concentration, indicating an almost 100% SO_2 removal efficiency. Therefore, SO_2 was accumulated gradually in aqueous solution. Although the O_2 concentration of two campaigns was about 18%, SO_3^{2-} was still observed, as shown in Figure 4. SO_3^{2-} was gradually reacted with oxygen to form SO_4^{2-}. Furthermore, SO_3^{2-} and

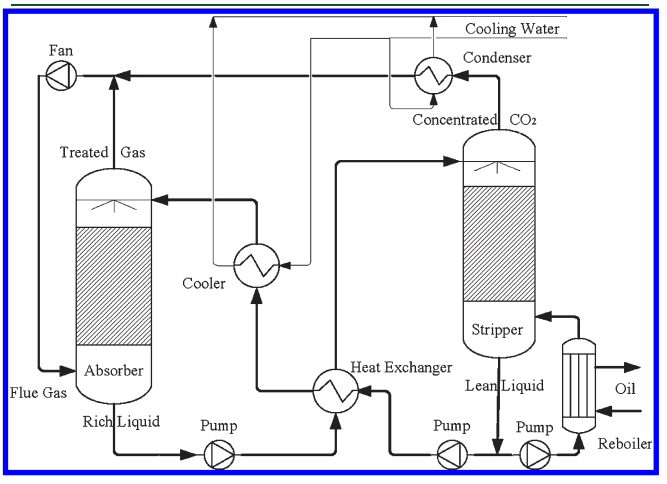

Figure 1. Flow diagram of the experimental system.

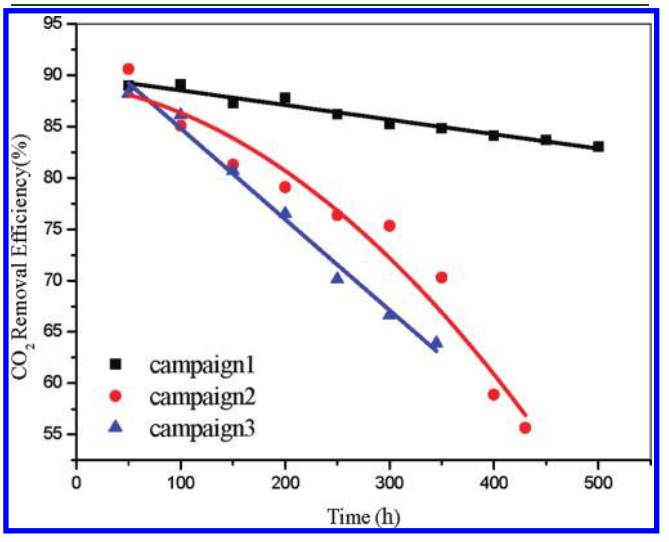

Figure 2. CO_2 removal efficiency changes with time.

Table 1. Experimental Conditions

	CO_2, vol %	O_2, vol %	SO_2, × 10^{-6}	amine cncn, mol/L	flue gas flow rate, Nm^3/h	operating time, h
campaign 1	11.89	18.2	0	4.64	86.12	500
campaign 2	11.86	17.8	214	4.57	82.83	430
campaign 3	12.26	18.1	317	4.44	83.41	345

dx.doi.org/10.1021/ef2010496 |*Energy Fuels* 2011, 25, 5802–5809

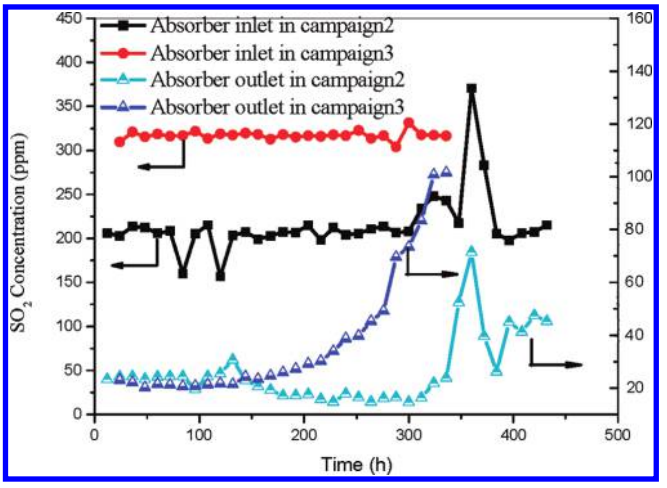

Figure 3. SO_2 concentration of the absorber.

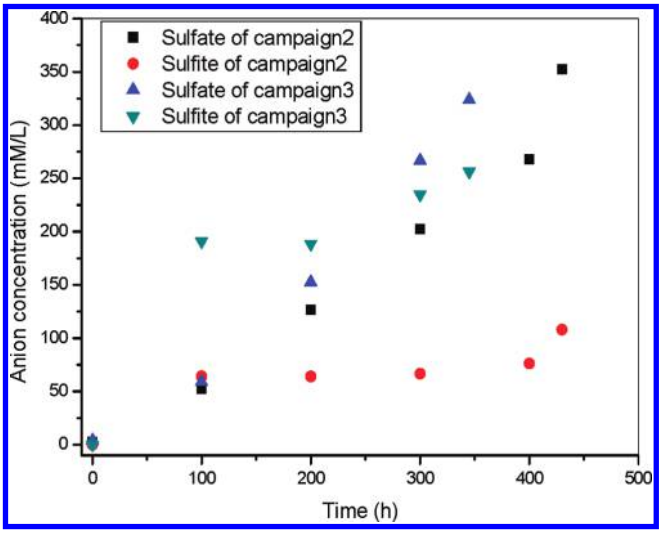

Figure 4. Sulfate and sulfite concentration of the two campaigns.

SO_4^{2-} concentrations climbed slowly as the SO_2 concentration increased.[15]

3.2. Amine Degradation. Solvent degradation is a serious problem associated with the chemical absorption of CO_2 from coal-fired power plant flue gas streams, caused by SO_2 and O_2, as well as by heating the solution for desorption. Campaign 1 evaluated the influence of both O_2 and temperature on the degradation of the absorbent. Campaigns 2 and 3 evaluated the contribution of SO_2 to absorbent degradation by comparison with campaign 1. The effect of the above-mentioned factors on the amine concentration are graphically illustrated in Figure 5. For the amine$-H_2O-CO_2-O_2$ system in campaign 1, the amine concentration was reduced from the initial 4.6 to 4.3 mol/L over 500 h, a decrease of 6.5%. For the amine$-H_2O-CO_2-O_2-SO_2$ system, however, it is decreased by 11.82% over 430 h and 34.7% over 345 h for campaigns 2 and 3, respectively. That is to say, with the increasing of SO_2 concentration, the tendency of amine degradation was accelerated. The SO_2 in the simulated flue gas may compete with CO_2 to react with amine, which retarded the CO_2 inhibited role in amine degradation and caused an increase of amine degradation.[16] The decrease of amine

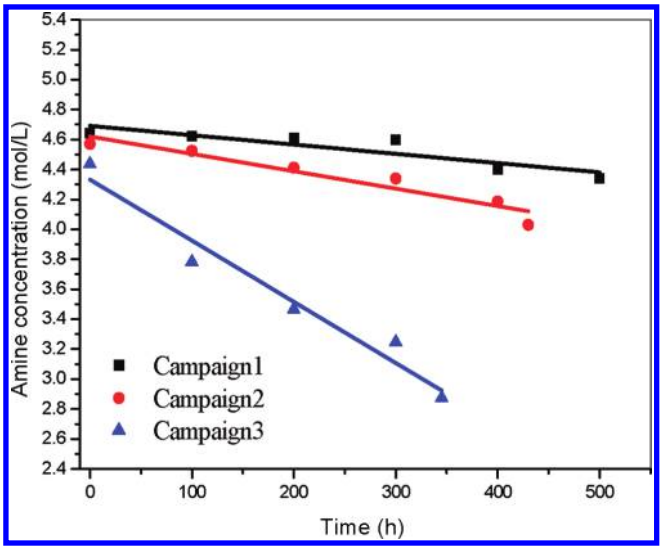

Figure 5. Amine degradation in the three campaigns.

concentration will directly reduce the chemical reaction rate as well as the CO_2 removal efficiency.

With the amine degradation, the total heat stable salts (HSS) were gradually accumulated in amine solutions. Four kinds of organic acid salts were detected, as shown in Figures 6 and 7; they are formate, acetate, oxalate, and glycolate. The pilot test results show that the formate and acetate were the main products of amine degradation for campaign 1, without SO_2. For campaign 2, with 214 ppm SO_2, they are formate and glycolate. Sulfate and sulfite were also observed in Figure 7 because SO_2 was continuously absorbed. The cases with other run times have similar results. Figure 8 shows the mass percent of HSS, only including the four kinds of organic acid salts mentioned. The concentrations and species of HSS can be used to evaluate the solvent degradation extent and possible degradation mechanisms. For campaign 1, the new absorbent contained approximately 0.14 mass % HSS after operating 500 h. However, for campaigns 2 and 3, this value was 0.98 mass % for 430 h and 0.92 mass % for 345 h, respectively. The accumulation rates of HSS for campaigns 1, 2, and 3 are 2.8, 22.8, and 26.7 mg/(kg h), respectively. It can be concluded that SO_2 accelerated the process of HSS accumulation, which agreed very well with the results shown in Figure 5.

3.3. Reaction Rate for CO_2 Absorption. As an acidic gas, SO_2 will combine with active amine, resulting in the reduction of free amine. Figure 9 shows the reduction of free amine at the outlet of stripper for the three campaigns. For campaign 1, although CO_2 lean loading is small, part of the active amine is still combined with it, which leads to the free amine concentration decreases. This part can be controlled by adjusting the re-boiler duty on the basis of the acceptable energy consumption. For campaigns 2 and 3, SO_3^{2-} and SO_4^{2-} ions combine with amine and cannot be regenerated under high pH value. Therefore, more and more free amine disappears. This tendency is accelerated as more SO_2 is absorbed, although SO_2 decreases the CO_2 lean loading.[12] This may be another reason for the reduction of the CO_2 removal efficiency.

For the absorption of CO_2 into amine aqueous solution, the reaction of CO_2 with H_2O is usually neglected in the overall CO_2 reaction rate expression. According to eq 2, the overall CO_2

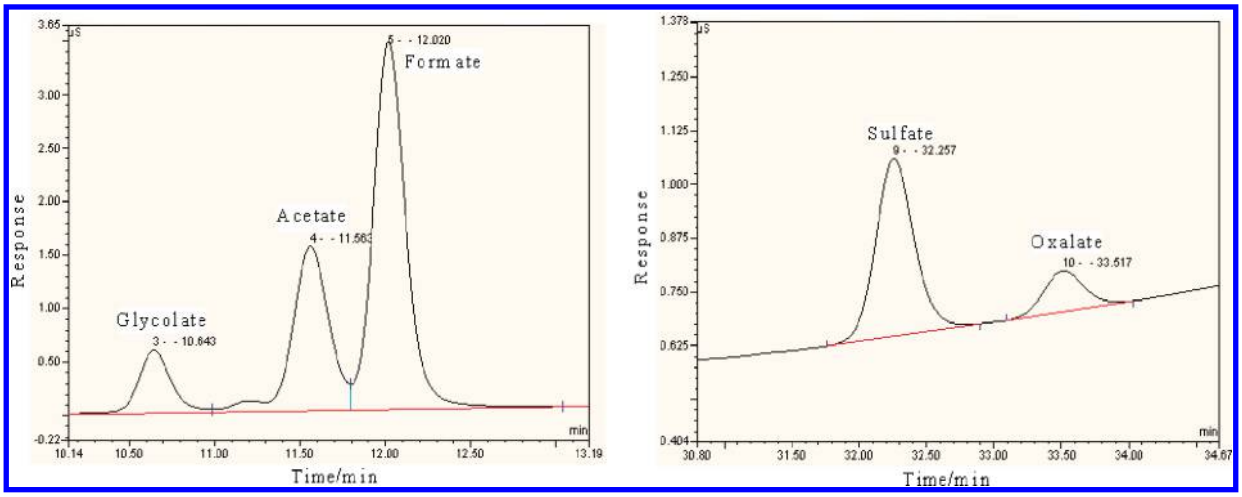

Figure 6. Anion chromatogram of campaign 1 around 500 h.

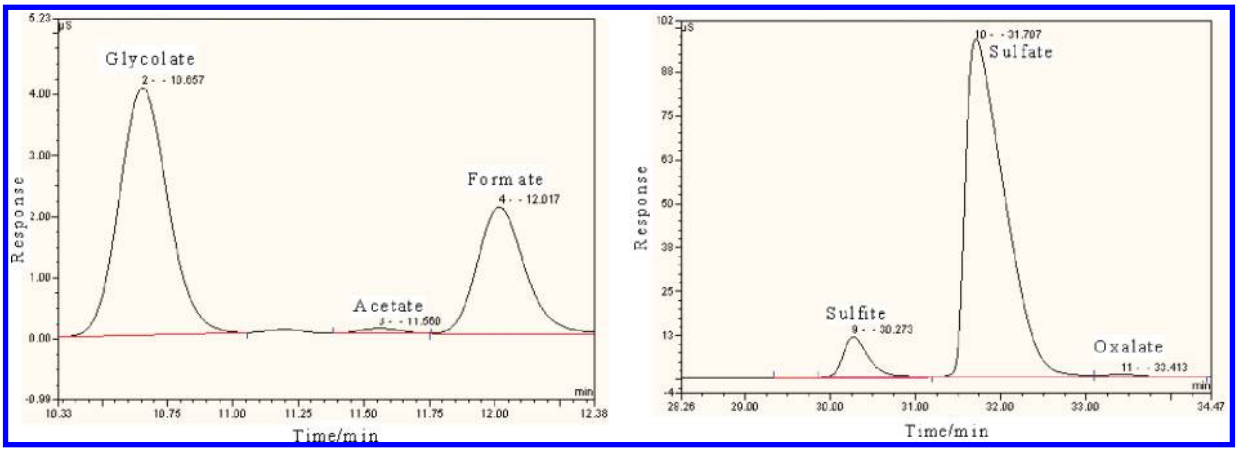

Figure 7. Anion chromatogram of campaign 2 around 300 h.

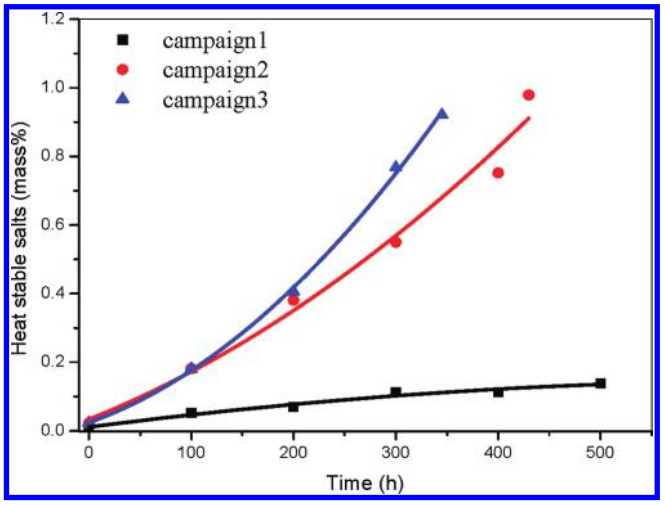

Figure 8. Effect of SO_2 on heat stable salts formation.

reaction rate constant, k_{ov}, can be expressed as the following equation:

$$k_{ov} = k_{am}[AM] + k_{OH^-}[OH^-] \quad (3)$$

The apparent reaction rate constant, k_{app}, is defined as follows:

$$k_{app} = k_{ov} - k_{OH^-}[OH^-] = k_{am}[AM] \quad (4)$$

$$[OH^-] = \frac{K_W}{K_P}\left(\frac{1-\alpha}{\alpha}\right), \alpha \geq 10^{-3}$$

$$[OH^-] = \sqrt{\frac{K_W}{K_P}[AM]}, \alpha \leq 10^{-3} \quad (5)$$

The $[OH^-]$ concentration was estimated from eq 5, given by Astarita et al.,[13,14] where α is the CO_2 loading in amine solution, K_P is the amine protonation constant, and K_W is the water dissociation constant. The kinetic data for CO_2 absorption of the three campaigns are shown in Table 2. The k_{ov} and k_{app} parameters are calculated using eqs 3 and 4, respectively. The overall CO_2 reaction rate constant, k_{ov}, as well as the apparent reaction rate constant, k_{app}, decreased with the reaction time, especially in campaigns 2 and 3. The main reason is the free amine decreases, as analyzed above. It was observed obviously that the k_{ov} and k_{app} values of campaign 1 are larger than those for campaigns 2 and 3, except for a small fluctuation from temperature changes. This is due to the k_{ov} and k_{app} increase with the increase of the amine concentration and solution temperature. All the calculated results agree with the experimental results.

dx.doi.org/10.1021/ef2010496 |*Energy Fuels* 2011, 25, 5802–5809

3.4. Mass Transfer. The information on the fundamental mass transfer characteristics of the CO_2 capture process were extracted by calculating the volumetric overall mass transfer coefficient ($K_G a_e$), mass transfer flux (N_A), liquid-side mass transfer coefficient (k'_g), and overall mass transfer coefficient (K_G). The following sections will introduce the determination of each value.

3.4.1. Volumetric Overall Mass Transfer Coefficient. The flux of element A (N_A) transferring from a gas stream to a liquid bulk at a steady state can be expressed in terms of the overall mass transfer coefficient (K_G), total system pressure (P), and equilibrium mole fraction of component A in gas phase (y_A^*) as follows:

$$N_A = K_G P(y_A - y_A^*) \tag{6}$$

considering the mass balance of the element in a packed column with height dz, which can be given as

$$N_A a_e \, dz = G_I \, d\left(\frac{y_A}{1 - y_A}\right) \tag{7}$$

where G_I represents the inert gas molar flow rate per cross-sectional area of the absorption column. By substituting the eq 6 into eq 7, it follows:

$$K_G a_e P(y_A - y_A^*) \, dz = G_I \, d\left(\frac{y_A}{1 - y_A}\right) \tag{8}$$

where $K_G a_e$ denotes the volumetric overall mass transfer coefficient. Figure 10 shows the absorber $K_G a_e$ value varied with time, for the three campaigns. Many factors have an effect on the $K_G a_e$ value, such as gas and liquid flow rate, CO_2 partial pressure and loading, liquid temperature, and solvent concentration.[17] The former three factors are almost constant during the CO_2 capture process for three campaigns in this work, and the CO_2 loading and the liquid temperature have small fluctuations during the campaigns, which can be ignored. Thus, Figure 10 shows that the free amine concentration is proportional to the $K_G a_e$ for the three campaigns. For campaign 1, the amine degradation and CO_2

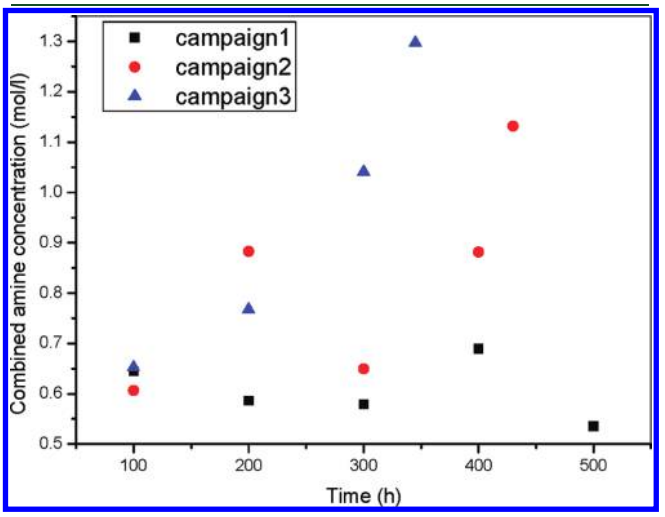

Figure 9. Amine combined with CO_2 and SO_2.

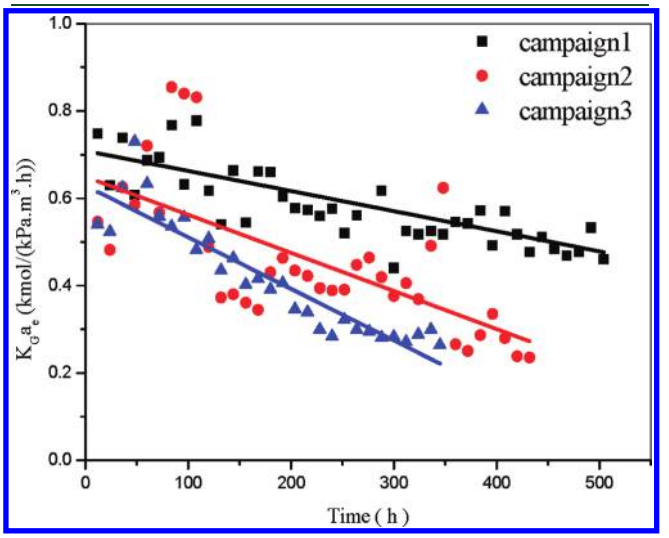

Figure 10. Volumetric overall mass transfer coefficient of the absorber.

Table 2. Kinetic Data for the Absorption of CO_2

	time, h	temp., °C	$H_{CO_2,L}$, kPa m^3/kmol	$[OH^-]10^5$, kmol/m^3	k_{ov}, s^{-1}	k_{app}, s^{-1}
campaign 1	0	44.2	5568.6	4.0	67004.5	67003.2
	100	42.6	5935.4	3.9	19258.0	19256.8
	200	41.2	5737.9	4.1	19872.6	19871.5
	300	41.1	5774.3	4.2	19869.5	19868.4
	400	41.3	5800.2	3.3	15648.9	15648.0
	500	41.8	5785.8	4.0	19677.0	19675.9
campaign 2	0	43.5	5485.0	4.1	68034.2	68033.0
	100	43.5	6261.8	4.1	22923.6	22922.3
	200	45.0	6940.6	2.7	13971.3	13970.4
	300	43.9	6586.3	3.7	19769.0	19767.8
	400	43.6	7013.5	2.4	11581.9	11581.1
	430	44.3	7734.2	1.7	7158.8	7158.2
campaign 3	0	44.9	5590.3	3.1	69184.7	69183.6
	100	44.9	6588.1	3.1	15234.2	15233.1
	200	45.0	6854.2	2.3	9583.9	9583.1
	300	44.9	7566.8	1.4	4458.3	4457.8
	345	44.7	8162.7	0.8	1803.0	1802.8

dx.doi.org/10.1021/ef2010496 |*Energy Fuels* 2011, 25, 5802–5809

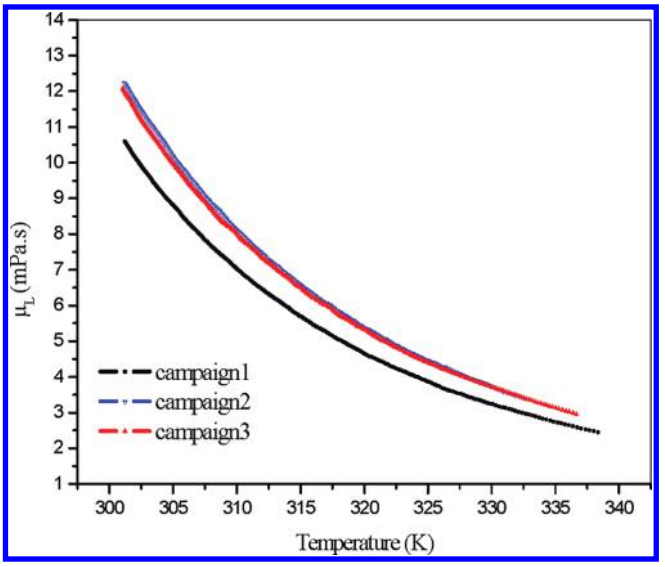

Figure 11. Viscosities of the fresh amine solution for the three campaigns.

loading together result in the $K_G a_e$ decreases. For campaigns 2 and 3, however, the SO_2 loading also plays an important role in the $K_G a_e$ decreases.

3.4.2. Liquid-Side Mass Transfer Coefficient. It is often appropriate to consider amine reactions as first order in CO_2 concentration and amine concentration. Under normal conditions, all species except CO_2 are assumed to be a nearly constant concentration across the liquid boundary layer, and the reaction rate can be represented by a pseudo-first-order rate constant, k_1. Then, the following approximation is valid:[18,19]

$$k_g' = \frac{\sqrt{D_{CO_2,L}(k_2 C_{am})}}{H_{CO_2,L}} \quad (9)$$

where the pseudo-first-order rate constant is replaced by a second order rate constant multiplied by the amine concentration in the bulk solution. $D_{CO_2,L}$ and $H_{CO_2,L}$ are the diffusion coefficient and the Henry's law constant for CO_2 in liquid solution, respectively.

The $D_{CO_2,L}$ was calculated from the following equations:[20]

$$D_{CO_2,L} = D_{CO_2,W}\left(\frac{\mu_W}{\mu_L}\right)^{0.8} \quad (10)$$

$$D_{CO_2,W} = 2.35 \times 10^{-6} \exp\left(\frac{-2119}{T}\right) \quad (11)$$

The viscosities of fresh solutions were continuously measured, with temperature decreases, by means of SV-10 viscometers; they ranged from 0.3 to 10 000 mPa s. The accuracy of the viscosities was estimated to be ±3%. The results are shown in Figure 11. The viscosities of the three campaigns decrease as the temperature increases. The amine concentration has an effect on the small differences in the viscosities between three campaigns.

The Henry's law constant for CO_2 is obtained using the following correlation:[21]

$$\log H_{CO_2,L} = \log H^* + (h_+ + h_- + h_g)I \quad (12)$$

$$\ln H^* = a + \frac{b}{T} + \frac{c}{T^2} \quad (13)$$

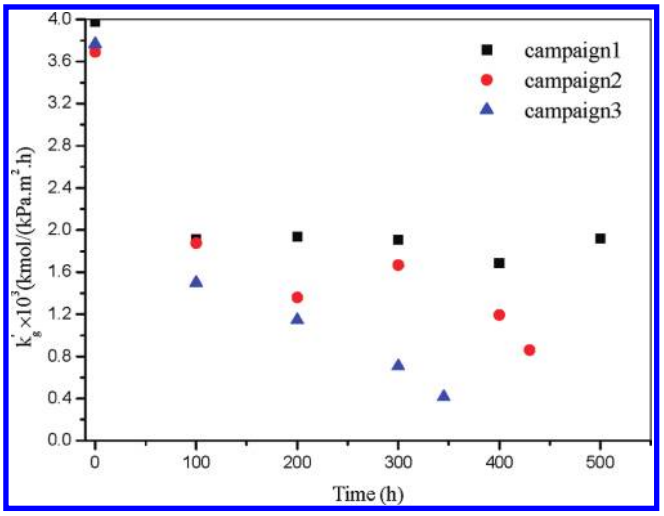

Figure 12. Liquid-side mass transfer coefficient of the three campaigns.

where $H_{CO_2,L}$ and H^*, as a function of temperature and amine concentration, are the Henry constants for the electrolyte solution and the pure molecular solvent, respectively. h_+ and h_- are the van Krevelen coefficients for the cations and anions in solution, and h_g is the coefficient for the dissolving gas. Additionally, a, b, and c are fitting constants from experimental data. I is the ionic strength of the solution, given by eq 14.

$$I = \left(\frac{1}{2}\right)\sum C_i Z_i^2 \quad (14)$$

Here, C_i and Z_i are the concentration and charge of species i, respectively. The relevant results were shown in Table 2. As for campaign 2 and campaign 3, the Henry constant increased with the accumulation of SO_3^{2-} and SO_4^{2-} ions because the ionic strength of the solution increased as SO_2 absorbed gradually. It directly leads to the liquid-side mass transfer coefficient decreased.

In effect, the viscosities of solutions vary as SO_2 loading increases, amine degrades, and temperature changes. It assumes that the viscosities do not vary with loading and amine concentration for qualitative analysis. Thus, the liquid-side mass transfer coefficient is only a function of temperature and the Henry constant. As shown in Figure 12, the k'_g decreased with the reaction time for the three campaigns, and from campaign 1 to campaign 3, the k'_g decreased as the SO_3^{2-} and SO_4^{2-} concentrations increased. The decrease rate is also comparably slow. According to equation8, one of the reasons is the increase in the Henry constant. The main reason is the active amine decrease caused by amine degradation and SO_2 and CO_2 combination with amine. This result is also in good agreement with the analysis of the k_{ov} and k_{app}.

3.4.3. Overall Mass Transfer Coefficient. For deep analysis, the mass transfer flux, N_{CO2}, was calculated on the basis of the pilot experimental results in the gas-side. The calculated results are shown in Figure 13. The mass transfer flux of campaign 1 decreases slightly during the campaign. For campaigns 2 and 3, however, after addition of SO_2, the reduction rates of mass transfer flux were accelerated. The results indicate that the SO_2 loaded in the amine solution decreases the absorption rate of CO_2. It is also good agreement with all of the above analyses.

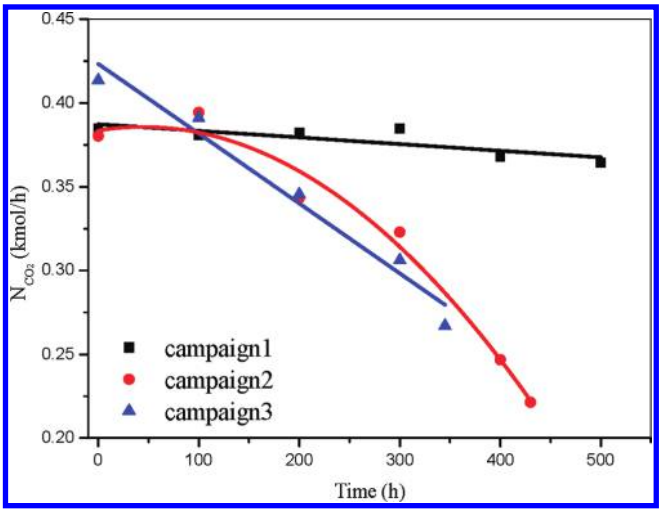

Figure 13. Mass transfer performance under different conditions.

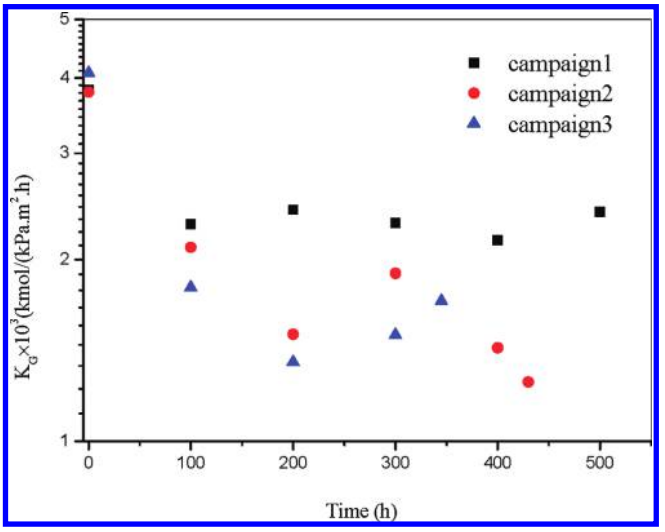

Figure 14. Overall mass transfer coefficient for the three campaigns.

Furthermore, the overall mass transfer coefficient was calculated by using the following equation:

$$K_G = \frac{N_{CO2}}{a_e \pi r^2 h \Delta P_{CO2}} \tag{15}$$

where r is the semi-diameter of the absorber column (m) and h is the height of packing (m). ΔP_{CO_2} (kPa) is defined as follows:

$$\Delta P_{CO2} = \frac{(P_{CO_2,\,in} - P^*_{CO_2,\,in}) - (P_{CO_2,\,out} - P^*_{CO_2,\,out})}{\ln\left(\frac{P_{CO_2,\,in} - P^*_{CO_2,\,in}}{P_{CO_2,\,out} - P^*_{CO_2,\,out}}\right)} \tag{16}$$

where $P_{CO_2,in}$ and $P_{CO_2,out}$ represent the partial pressure of CO_2 at the bottom and the top of the absorber, respectively. $P^*_{CO_2,in}$ and $P^*_{CO_2,out}$ represent the partial pressure of CO_2 in equilibrium with the liquid bulk at the inlet and the outlet of the absorber, respectively.

In a packed column for gas-absorption, it is more practical to present rates of absorption in terms of transfer coefficients based on a unit volume of the absorption column, as follows:

$$\frac{1}{K_G a_e} = \left(\frac{1}{k_G a_e}\right) + \left(\frac{1}{k'_g a_e}\right) \tag{17}$$

From this equation, plotting the known $(1/K_G a_e)$ values in Figure 10 against the corresponding $(1/k'_g)$ ratio at the same time provides a straight line of which the slope directly represents the reciprocal of effective area $(1/a_e)$.[17]

The overall mass transfer coefficient of the three campaigns was given in Figure 14. The K_G of campaign 1 has a small fluctuation. Considering the fitting straight line of campaign 1, the K_G value has small reduction with reaction time. The absolute slope value of the fitting straight line gradually climbs from campaign 1 to campaign 3. This means that the overall mass transfer resistance was increased with the SO_2 accumulation in the amine solution. Thus, it is easy to know that the absorption rate of CO_2 was declined in the presence of SO_2.

4. CONCLUSIONS

A pilot plant for CO_2 capture from coal-fired power plants was built in Tsinghua University. The pilot plant adopts amine-based chemical absorption process, including absorption and desorption. The gases out of the absorber and stripper were fed back to the absorber again, as well as the condensate. The whole system, therefore, is closed, which can keep the gas and water balance.

The major work of this paper is to test the cyclic CO_2 capture performance and chemical stability of new absorbent in the pilot plant with the presence of SO_2 for a long period. Three campaigns were conducted. The flue gas of campaign 1 contains about 12 vol % CO_2 and 18 vol % O_2. The experimental conditions of campaigns 2 and 3 were identical to those of campaign 1, except for adding SO_2 at 214 and 317 ppm, respectively.

The results indicate that SO_2 was accumulated gradually in new absorbent, and the SO_2 removal efficiency is almost 100%. The CO_2 removal efficiency decreases gradually as circulating time increases because active amine decreases. This trend was accelerated with the addition of SO_2. Compared with thermal and oxidative degradation, the addition of SO_2 aroused more serious amine degradation. The pilot test results show four kinds of organic acid salts, formate, acetate, oxalate, and glycolate, that were detected in the three campaigns. The formate and acetate were the main products of amine degradation for campaign 1 without SO_2. For campaign 2 and 3 with SO_2, they are formate and glycolate. The results of amine degradation and HSS formation are in accordance with previously-mentioned results.

The analysis of mass transfer and CO_2 reaction rate suggests that the changing tendency with time of the overall CO_2 reaction rate constant k_{ov}, the apparent reaction rate constant k_{app}, the volumetric overall mass transfer coefficient $K_G a_e$, and the liquid-side mass transfer coefficient k'_g, and so on are similar, which is in proportion to the free amine concentration. The amine degradation and lean CO_2 loading decrease the active amine concentration for campaign 1. For campaigns 2 and 3, SO_2 combined with amine result in further decreases of the free amine.

AUTHOR INFORMATION

Corresponding Author

*Tel.: +86-10-62788668. Fax: +86-10-62770209. E-mail: wangshuj@tsinghua.edu.cn.

■ ACKNOWLEDGMENT

This work was a collaboration research project between Tsinghua University and Toshiba.

■ NOMENCLATURE

a_e = effective interfacial area per unit volume of packing(m^2/m^3).
C_{in} = gas phase CO_2 concentration at the bottom of absorber (%).
C_{out} = gas phase CO_2 concentration at the top of absorber (%).
C_{am} = concentration of amine in the liquid phase ($kmol/m^3$).
$D_{CO_2,L}$ = the diffusion coefficient of CO_2 in amine solution (m^2/s).
$D_{CO_2,W}$ = the diffusion coefficient of CO_2 in water (m^2/s).
G_I = inert molar gas load ($kmol/(m^2\ h)$).
$H_{CO_2,L}$ = Henry's law coefficient of CO_2 in amine solution ($kPa\ m^3/\ kmol$).
h = packing height (m).
k_{am} = second order rate constant of amine ($m^3/kmol\ s$).
k_{OH^-} = reaction rate constant for CO_2 hydration ($m^3/kmol\ s$).
k_{ov} = the overall CO_2 pseudo-first-order reaction rate constant (s^{-1}).
k_{app} = the apparent reaction rate constant (s^{-1}).
K_G = overall mass transfer coefficient ($kmol/(m^2\ h\ kPa)$).
k_G = gas-side mass transfer coefficient ($kmol/(m^2\ h\ kPa)$).
k'_g = liquid-side mass transfer coefficient ($kmol/(m^2\ h\ kPa)$).
N_{CO_2} = mass transfer flux of the absorbed component CO_2 ($kmol/(m^2\ h)$).
P = total pressure (kPa).
ΔP_{CO_2} = average partial pressure of CO_2 (kPa).
r_{ov} = the overall CO_2 reaction rate ($kmol/m^3\ s$).
y_A = mole fraction of component A in gas bulk (mol/mol).
y^*_A = gas-phase mole fraction of component A in equilibrium with the concentration of component A in the liquid phase (mol/mol).

Greeks
μ_L = viscosity of amine solution (mPa s).
μ_W = viscosity of water (mPa s).
η_{CO_2} = CO_2 removal efficiency (%).

■ REFERENCES

(1) Desideri, U.; Paolucci, A. *Energy Convers. Manage.* **1999**, *40*, 1899–1915.
(2) Rao, A. B.; Ruben, E. S. *Environ. Sci. Technol.* **2002**, *36*, 4467–4475.
(3) Singh., D.; Croiset, E.; Douglas, P. L.; Douglas, M. A. *Energy Convers. Manage.* **2003**, *44*, 3073–3091.
(4) Kolbitsch, P.; Pröll, T. ; Bolhar-Nordenkampf, J.; Hofbauer, H. *Energy Procedia* **2009**, *1*, 1465–1472.
(5) Konduru, P. B.; Vaidya, P. D.; Kenig, E. Y. *Environ. Sci. Technol.* **2010**, *44*, 2138–2143.
(6) Darde, V.; Thomsen, K.; van Well, W. J. M.; Stenby, E. H. *Energy Procedia* **2009**, *1*, 1035–1042.
(7) Rochelle, G. T. *Science* **2009**, *325*, 1652–1654.
(8) Idem, R.; Wilson, M.; Tontiwachiwuthikul, P.; Chakama, A.; Veawab, A.; Aroonwilas, A.; Gelowitz, D. *Ind. Eng. Chem. Res.* **2006**, *45* (8), 2414–2420.
(9) Chen, X.; Closmann, F.; Rochelle, G. T. *Energy Procedia* **2011**, *4*, 101–108.
(10) Uyanga, I. J.; Idem, R. O. *Ind. Eng. Chem. Res.* **2007**, *46* (8), 2558–2566.
(11) Strazisar, B. R.; Anderson, R. R.; White, C. M. *Energy Fuels* **2003**, *17* (4), 1034–1039.
(12) Gao, J. B.; Wang, S. J.; Zhou, S. *Proc. CSEE* **2011**, *31* (5), 52–57.
(13) Xiao, J; Li, C. W.; Li, M. H. *Chem. Eng. Sci.* **2000**, *55*, 161–175.
(14) Sun, W. C.; Yong, C. B.; Li, M. H. *Chem. Eng. Sci.* **2005**, *60*, 503–516.
(15) Gao, J. B.; Wang, S. J.; Zhou, S.; Zhao, B.; Chen, C. *Energy Procedia* **2011**, *4*, 1534–1541.
(16) Wappel, D.; Khan, A.; Shallcross, D.; Joswig, S.; Kentish, S.; Stevens, G. *Energy Procedia* **2009**, *1*, 125–131.
(17) Adisorn, A.; Paitoon, T. *Ind. Eng. Chem. Res.* **1998**, *37* (2), 569–575.
(18) Cullinane, J. T.; Rochelle, G. T. *Chem. Eng. Sci.* **2004**, *59* (17), 3619–3630.
(19) Cullinane, J. T.; Rochelle, G. T. *Ind. Eng. Chem. Res.* **2006**, *45* (8), 2531–2545.
(20) Versteeg, G. F.; Van Swaaij, W. P. M. *J. Chem. Eng. Data* **1988**, *33*, 29–34.
(21) Browning, G. J.; Weiland, R. H. *J. Chem. Eng. Data* **1994**, *39* (4), 817–822.